

Study of Corrosion Behavior of Arc Sprayed Aluminum Coating on Mild Steel

Erfan Abedi Esfahani, Hamidreza Salimijazi, Mohamad A. Golozar, Javad Mostaghimi & Larry Pershin

Journal of Thermal Spray Technology

ISSN 1059-9630

Volume 21

Number 6

J Therm Spray Tech (2012)

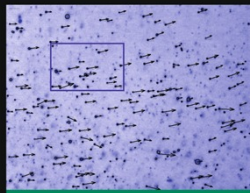
21:1195-1202

DOI 10.1007/s11666-012-9810-x

Volume 21 Number 6 • December 2012

TSS
ASM Thermal Spray Society
An Affiliate Society of ASM International

JOURNAL OF Thermal Spray TECHNOLOGY®



INSIDE:

- Nanostructured Ceramic Bondcoat for Improved Adhesion on Smooth Metal Substrate
- Solution-Precursor and Suspension Thermal Spray Coatings with Engineered Microstructures and Properties
- Tribological B₄C Coatings by Vacuum Plasma Spraying
- Simulation of Impacts of Partially Molten Particles
- Plasma Sprayed Apatite-Lanthanum Silicate Coatings for Solid Oxide Fuel Cell Application
- and much more....

Christian Moreau
Editor-in-Chief

Erick Meillot
Guest Editor

Special Issue: 5th International Workshop on Suspension and Solution Thermal Spraying (S2TS) 2011



 Springer

11666 • ISSN 1059-9630
21(6) 1099-1362 (2012)

 ASM INTERNATIONAL
The Materials Information Society

Available online
www.springerlink.com

Your article is protected by copyright and all rights are held exclusively by ASM International. This e-offprint is for personal use only and shall not be self-archived in electronic repositories. If you wish to self-archive your work, please use the accepted author's version for posting to your own website or your institution's repository. You may further deposit the accepted author's version on a funder's repository at a funder's request, provided it is not made publicly available until 12 months after publication.



Study of Corrosion Behavior of Arc Sprayed Aluminum Coating on Mild Steel

Erfan Abedi Esfahani, Hamidreza Salimijazi, Mohamad A. Golozar, Javad Mostaghimi, and Larry Pershin

(Submitted January 25, 2012; in revised form June 28, 2012)

In the current study, aluminum coating was deposited on mild steel by arc spraying. A well-adhered coating with low level of porosity was successfully obtained. To evaluate the corrosion behavior of the coating, electrochemical impedance spectroscopy (EIS) and polarization tests in 3.5% NaCl solution were carried out. The as-coated samples were also subjected to a 1500-h salt spray assay. Polarization tests indicated that the corrosion current density of the aluminum coating is more than that of bulk aluminum. This could be due to the penetration of the electrolyte through open pores, resulted in the acceleration of aluminum corrosion. EIS measurements showed that the corrosion performance of the coating is improved during a long time immersion and exposure to saline mist. This could be due to plugging of pores by corrosion products which hinder further penetration of the electrolyte through the coating. The results obtained indicated that twin wire arc sprayed aluminum coatings can reliably protect steel structures against corrosion in chloride-containing aqueous solutions.

Keywords Aluminum coating, Wire arc spray, Corrosion, Electrochemical impedance spectroscopy

1. Introduction

Plain carbon steels are widely utilized in structures because of their suitable mechanical properties, good performance, and low cost. However, in some harsh conditions such as seashore environment with high humidity and salt particles, corrosion of carbon steels becomes a major concern and thus their applications would be limited.

Up to now, protection of steel structures against corrosion degradation instead of using more resistant bulk materials, which would bring a significant cost issue, has been the main objective of extensive research. It would reduce costs by preserving the structure and increasing its service life (Ref 1). Anodic (Ref 2) and cathodic protections (Ref 3), metallic coatings (Ref 1, 4, 5), paintings (Ref 6-9), and inhibitors (Ref 10, 11) are some of the most used methods in order to delay and/or to reduce corrosion.

An effective way to improve the corrosion resistance of steel is to use protective coatings on surfaces. A wide variety of metallic coatings are used for this purpose. The most commonly used metals for protection of steel against

corrosion are anodic to substrate such as zinc, aluminum, and zinc/aluminum which eliminate the need for completely pinhole-free barriers (Ref 4, 12, 13).

Numerous methods exist for applying protective coatings, such as hot dip (Ref 4, 14, 15), physical vapor deposition (Ref 16, 17), chemical vapor deposition (Ref 18, 19), and various thermal spray methods. Amongst various types of spray processes, twin wire arc spray is widely used for deposition of anti-corrosion coatings. This is due to its economical advantages and high deposition rate (Ref 20) compared with other coating processes. It can also be used as a mobile unit to coat complex and large steel structures such as vessels, bridges, and offshore platforms. Wire arc spray is a process which utilizes two wires as consumable arc electrodes, an electric arc melts the tips of the electrodes. The liquid metal is then atomized by a gas jet and projected towards the substrate. The molten droplets are spread and solidified upon the impact to the substrate forming so called “splats”. The coating can build up by laying the individual splats on top of each other (Ref 21).

Various corrosion tests have been performed to study the corrosion performance of the thermally sprayed aluminum. Han et al. (Ref 22) investigated the corrosion behavior of the thermal sprayed aluminum and the effect of its thickness on STS 304 using polarization tests in seawater. They found that thermal sprayed aluminum coatings act as a sacrificial protection to the substrate. They also showed that the coating with higher thickness represent a better corrosion resistance in seawater. Chaliampalias et al. (Ref 23) and Rodriguez et al. (Ref 24) also used salt spray tests to show that thermal sprayed aluminum coatings could protect low carbon steels from corrosion in chloride-containing atmospheres. Panossian et al. (Ref 12) and Schmidt et al. (Ref 25) used field tests in the marine atmosphere to investigate the corrosion

Erfan Abedi Esfahani, Hamidreza Salimijazi and Mohamad A. Golozar, Department of Materials Engineering, Isfahan University of Technology, 84156-83111 Isfahan, Iran; and Javad Mostaghimi and Larry Pershin, Centre for Advanced Coating Technologies, University of Toronto, Toronto M5S 3G8, Canada. Contact e-mail: e.abediesfahani@ma.iut.ac.ir, errffaan@gmail.com

behavior of aluminum coatings. Liu et al. (Ref 26) investigated the corrosion performance of the sealed aluminum arc sprayed coatings on 6061 aluminum alloy and found that hydrothermal sealing could improve the corrosion behavior of the coatings.

Despite the fact that large amount of work has been carried out in the field of thermally sprayed aluminum coating and its corrosion behavior, an evident gap in the knowledge exists: how and why the mechanism of the coating protection against corrosion changes. In the present work, the mechanism of the aluminum coating corrosion protection and its changes during long-term immersion in chlorine-containing solution was comprehensively investigated. Electrochemical impedance spectroscopy (EIS) was employed at different exposure times to study long-term protective performance of the arc sprayed aluminum coating on mild steel in 3.5% NaCl solution which is related to its sacrificial abilities as well as its barrier protection. Appropriate interpretation of EIS data with an equivalent circuit could provide detailed information on the corrosion process at the electrolyte/electrode interface. In order to study the corrosion resistance behavior of the wire arc coating during exposure of steel structures to chlorine-containing solutions, EIS measurements after salt spray assay were carried out. The results can be used to evaluate coatings barrier or pore resistance effects during exposure.

2. Experimental Procedure

2.1 Materials and Methods

Commercially available 99% aluminum wire with 1.6 mm in diameter was supplied by Sulzer-Metco Inc., (Westbury, NY, USA). Aluminum coating was deposited on mild steel sheets (Fe-0.05C-0.04Al-0.25Mn-0.01P-0.004S-0.01Si wt.%) using a twin wire arc spray system (ValuArc, also from Sulzer-Metco). Details of spraying process parameters are tabulated in Table 1.

Prior to the deposition, surfaces of substrates were grit blasted by white aluminum oxide to enhance the adhesion of the coating by means of mechanical interlocking mechanisms. The degree of cleanliness Sa3 was achieved by comparison with the surface quality standards of the NACE RM 01 70 code (Ref 27).

Table 1 Twin wire arc spray process parameters

Spray parameters	Unit
Coating material	99% Al
Wire diameter	1.6 mm
Nozzle type	HV cup
Air inlet pressure	586 kPa
Stand off distance	100 mm
Feed rate	82 g/min
Voltage	33 V
Current	200 A
Substrate temperature	Room temperature

2.2 Coatings Characterization

Cross sections of coatings were examined using scanning electron microscope (SEM, Philips XL 30) operated at 20 kV, equipped with an EDS tool for the elemental analysis. The porosity of the coatings was determined by image analysis software (Image Tool 3.00) using several SEM images.

Phase compositions of the coatings were analyzed by x-ray diffraction (XRD, Philips X'Pert-MPD) using Cu K α radiation ($\lambda = 1.54056 \text{ \AA}$) generated at 40 kV and 30 mA.

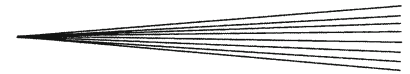
The adhesion strength between the coating and substrate is a major requirement for any coating to maintain its integrity under service conditions, it was measured based on ASTM-C633 standard (Ref 28).

2.3 Corrosion Tests

Tafel polarization tests were conducted in a conventional three-electrode cell with the sample as the working electrode, the platinum as the counter electrode, and saturated calomel electrode (SCE) as the reference. The working electrodes were cut (15 mm \times 15 mm) and electrical wires were soldered to the rear side of the coupons in order to allow electrochemical measurements. Samples were then embedded in an epoxy and the sprayed area of 1 cm² was left exposed to the electrolyte. The edges of the coupons were also masked using lacquer to avoid crevice corrosion. Prior to the corrosion tests, samples were washed in distilled water and ethanol, and then dried in warm air. All the measurements were done in 3.5 wt.% aqueous sodium chloride (NaCl) solution at room temperature under the static and natural aerated condition, using an AMETEK potentiostat (model PARSTAT2273) at the scan rate of 1 mV/s. Prior to polarization tests, specimens were kept in the solution for 3 h in order to establish the free corrosion potential (E_{corr}). The corrosion potentials as well as the corrosion current densities were extracted from the Tafel polarization plots.

EIS measurements were carried out to evaluate the coating properties for various immersion times up to 44 days. A corrosion cell was constructed by sticking a glass tube with an area of 7 cm² on the coated sample. The counter and reference electrodes were the same as Tafel polarization test. Impedance values were recorded in the frequency range from 100 kHz to 10 mHz under controlled potential conditions with an AC potential signal of 10 mV varied about the open-circuit potential. The impedance curves were fitted to the coating model using Zview software. Cross sections of the corroded samples were polished and examined by SEM after 44 days of immersion.

Standard neutral salt spray test was also performed to evaluate the corrosion resistance of the coated samples. The assay was conducted according to ASTM B 117/90 standard (Ref 29). The edges of the coated samples (75 mm \times 70 mm) were sealed using molten wax and then fixed on a plastic sample holder at an angle of 30° to vertical in the salt spray chamber. After 1500 h of the



exposure to the salt spray, specimens were also analyzed for their barrier or pore resistance using EIS measurement. To identify the corrosion products on the surface of the coatings, the coatings were analyzed by XRD technique.

3. Result and Discussion

3.1 Coatings Characterization

The XRD pattern of the coating is shown in Fig. 1. The only distinguishable phase is pure aluminum in the coating. No other minor phase could be detected due to their low concentration in the coating.

SEM micrograph of the cross section of the aluminum coating is shown in Fig. 2. The overall porosity percentage was around 7% and the coating thickness was about

150 μm . The overall oxide content was around 4%. A well-bonded coating to the substrate with no distinctive irregular interface can be observed in the micrograph. Bright and dark regions were identified in Fig. 2. Results obtained by EDS indicated that the chemical composition of the bright regions is 98 ± 1.1 at.% Al and 0.5 ± 0.1 at.% Fe and the chemical composition of the dark regions, which were marked by arrows, is 83 ± 0.9 at.% Al and 16 ± 0.6 at.% O. These results indicate that the dark regions contain more oxides coming from the in-flight particle oxidation during spraying.

The adhesion strength of the coatings was measured and results are tabulated in Table 2. All failures were occurred at the line of coating/substrate interface. The mean value of the adhesion strength was 27 MPa which is slightly higher than those reported somewhere else (Ref 21).

3.2 Corrosion Behavior

3.2.1 Tafel Polarization Tests. Figure 3 shows Tafel polarization plots (E - $\log i$) of the arc sprayed aluminum coating and steel substrate in 3.5% NaCl solution at room temperature under static and natural aerated conditions. The values of the corrosion potential (E_{corr}) and the corrosion current density (i_{corr}) were extracted from the curves using the Tafel extrapolation method. The E_{corr} values were -1030 and -610 mV_{SCE} for the aluminum coating and steel substrate, respectively. It is clear that the corrosion potential value of the steel substrate was more

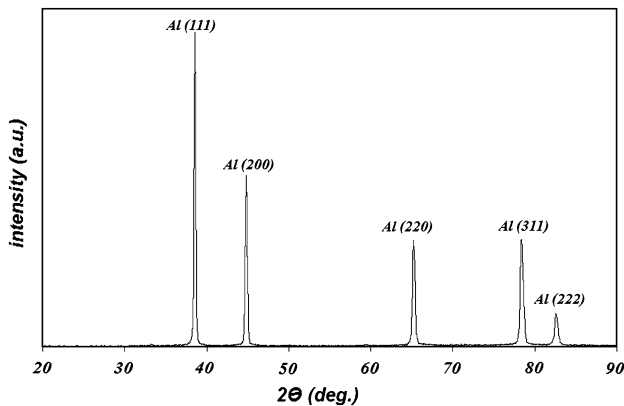


Fig. 1 XRD pattern of the as-sprayed aluminum coating

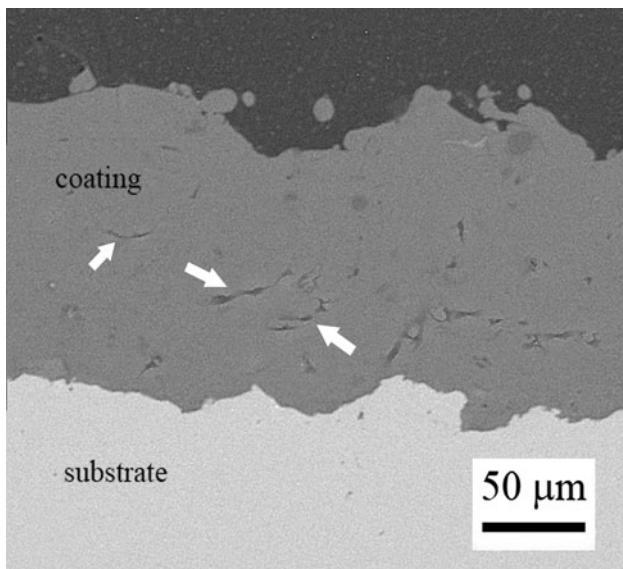


Fig. 2 The backscattered SEM micrograph of the cross section of aluminum coating. Arrows show oxide phases in the coating

Table 2 Bond adhesion strength of the arc sprayed coatings

Sample	1	2	3	4	Average
Bond strength, MPa	24	30	26	28	27 ± 3

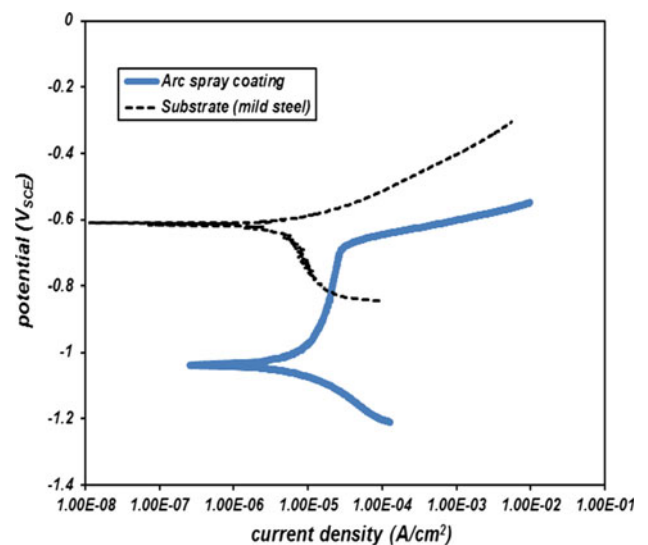


Fig. 3 Tafel polarization curves of mild steel substrate and aluminum arc sprayed coating in 3.5% NaCl solution

positive than that of aluminum coating. Thus, the corrosion of the aluminum coating can take place in preference to the corrosion of steel.

The i_{corr} values were 5 and 6 $\mu\text{A}/\text{cm}^2$ for the sprayed coating and steel substrate, respectively. The current density of the arc sprayed aluminum is higher than that of the bulk aluminum reported elsewhere (Ref 30). There is some level of interconnected porosity (7%) in the coating that allows the electrolyte to reach the substrate. This behavior has been seen in several other thermal spray coatings such as Al and Al/SiC composites on Mg by flame spray (Ref 31) and stainless steel sprayed by HVOF in NaCl solution (Ref 32), plasma sprayed $\text{Al}_2\text{O}_3 + \text{TiO}_2$ and NiCrAl coatings in H_2SO_4 solution (Ref 33). The development of the galvanic effects between these dissimilar materials at the coating/substrate interface leads to form galvanic corrosion. Since, the steel substrate is nobler than the aluminum coating; corrosion of aluminum coating would be accelerated and become higher than the corrosion current density of the bulk aluminum (Ref 34).

The coating showed a passive behavior (see Tafel plots in Fig. 3). The polarization curve of the coating exhibited a breakdown at higher anodic potentials, around $-700 \text{ mV}_{\text{SCE}}$. The presence of transpassivation point is due to the formation of pitting corrosion on the surface (Ref 26).

3.2.2 EIS of Coatings for Long Time Immersion. Figures 4 and 5 show the Nyquist and Bode plots of the arc sprayed aluminum coating for different immersion times in 3.5% NaCl solution, respectively. After 3 h of

exposure, two semi-circles on Nyquist plot (Fig. 4), and accordingly, two inflection points on the corresponding Bode phase plot can be distinguished (Fig. 5). It means that the system shows two time constants. The high-frequency loop corresponds to the coating, while the low-frequency loop can be attributed to the corrosion process (Ref 13, 34-36). The electrolyte which penetrated into the coating through the pores and splat boundaries caused the dissolution of the active zones inside the coating and generated capacitive loop at low frequencies. The electrolyte could also reach the substrate, but since the substrate is nobler than the coating, corrosion did not occur on steel. This type of spectra can be modeled by the equivalent circuit which was represented in Fig. 6. This equivalent circuit proposed for the two sub-electrochemical interfaces (Ref 13, 37). The equivalent circuit consists of a solution resistance (R_s) which relates to the test electrolyte between the working electrode and the reference electrode; a pair of elements of the pore resistance (R_{pore}) and the coating capacitance (C_{coat}) in parallel which relates to the coating defects. Their magnitudes can be extracted from the high-frequency loop on Nyquist plot. Another pair of elements; the charge transfer resistance (R_{ct}) and the double-layer capacitance (C_{dl}) in parallel can be related to the corrosion parameters and could be estimated from the low-frequency loop on Nyquist plot (Ref 13). Constant phase element (CPE) is commonly used to replace capacitance, because it hardly has pure capacitance in the real electrochemical process (Ref 37).

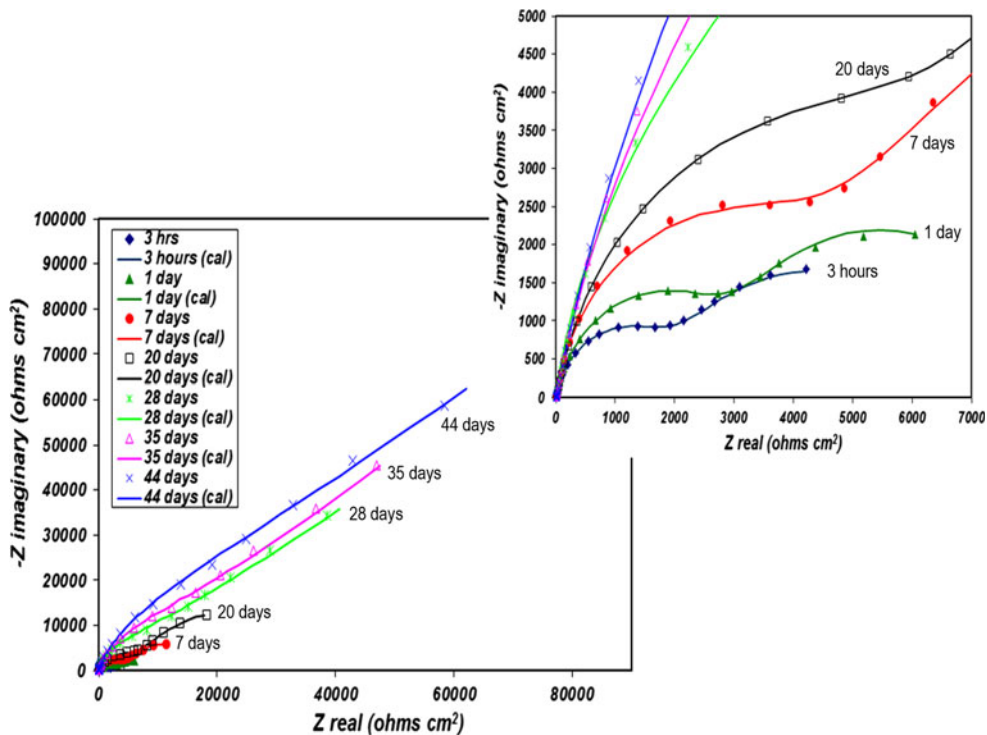


Fig. 4 Experimental and simulated Nyquist spectra of the aluminum coated steels in 3.5 wt.% NaCl solution using equivalent circuit shown in Fig. 6 and 7 for different exposure times



By increasing the immersion time more than 20 days, the style of Nyquist and Bode phase plots was changed and a straight line appeared at low frequencies instead of the capacitive loop on Nyquist plot. It has been reported that the straight line appears due to the Warburg

impedance created when the charge transfer is influenced by a semi-infinite length diffusion process (Ref 36). Under this condition, the equivalent circuit shown in Fig. 7 is useful for describing the electrochemical cell (Ref 34-38). Generally, the accumulation of the corrosion products in the pores of coatings leads to the appearance of Warburg behavior which causes the mass-transfer reaction (Ref 39, 40).

The EIS data were interpreted based on the proposed equivalent circuits using a suitable fitting procedure elaborated by Zview program software. Table 3 summarizes the circuit parameters using the fitting circuits in Fig. 6 and 7 and simulated spectra were shown in Fig. 4 and 5.

By increasing the immersion time, R_{pore} values increased. The E_{ocp} value was raised to $-854 V_{SCE}$ after 44 days of immersion, suggesting that pores within the coating were blocked due to the local accumulation of the corrosion products in the pores, which increased the pore resistance called "plugging effect" (Ref 31, 36, 38, 40). On the other hand, by increasing the immersion time more than 20 days, Warburg impedance decreased while R_{pore} increased up to 44 days. These two phenomena indicate that penetration of the electrolyte through the pores is restricted by increasing the immersion time due to the plugging effect (Ref 38).

Figure 8 shows the SEM micrograph of the cross section of the coating after 44 days of immersion. The coating is still well-adhered to the substrate and only some locally attacked areas can be observed (see arrows in Fig. 8) indicating that the penetration of the electrolyte through the coating pores can affect the electrochemical behavior of the sprayed coatings. Elemental analysis by EDS showed that the chemical composition of the dark region is 81 ± 0.9 at.% Al, 16 ± 0.6 at.% O, and 0.5 ± 0.1 at.% Cl. The dark regions contain oxides which formed during immersion. The oxide content of the coating increased during immersion, and was around 30% after 44 days of immersion. This aluminum oxide phase can act as a sealant for the coating porosity and passive layer to prevent further corrosion.

3.2.3 Salt Spray Tests. After 1500 h of exposure to saline mist, the aluminum deposited coating became darker (Fig. 9) due to the oxide film. Red iron corrosion product did not appear in the coating, confirming absence of steel (substrate) corrosion. A typical SEM cross-sectional micrograph of the Al-coated samples after salt spray assay is shown in Fig. 10. The corrosion of the specimen was not severe and was found in particular coating areas. The EDS analysis traced about 1 at.% chlorine and

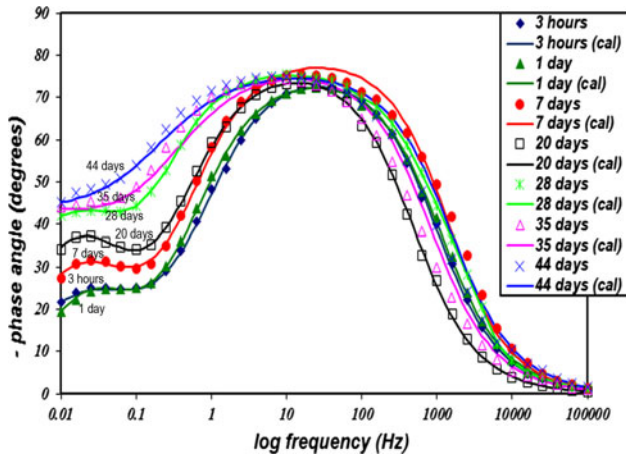


Fig. 5 Experimental and simulated Bode Phase spectra of the aluminum coated steels in 3.5% NaCl solution using equivalent circuit shown in Fig. 6 and 7 for different exposure times

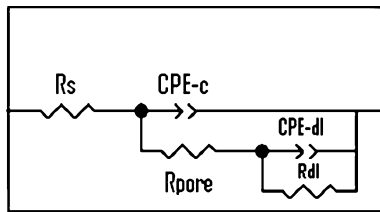


Fig. 6 Equivalent circuit for the coated sample after 3 h up to 20 days of immersion

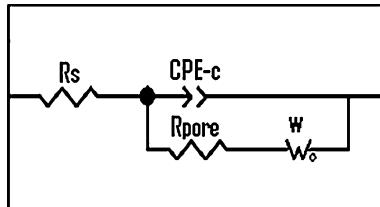


Fig. 7 Equivalent circuit for the coated sample after 20 days up to 44 days of immersion

Table 3 Electrochemical parameters obtained from the equivalent circuits simulation

Exposed time	E_{corr} , mV _{SCE}	R_s , Ω cm ²	CPE-c, μ F/cm ²	η_{CPE-c}	R_{pore} , Ω cm ²	CPE-dl, μ F/cm ²	η_{CPE-dl}	Rdl, Ω cm ²	W, μ /(cm ² Ω s ^{0.5})
3 h	-1,012	4.2	128	0.86	2,100	1571	0.71	4,900	...
1 day	-990	5.0	82	0.88	3,339	1499	0.82	5,040	...
7 days	-983	4.2	71	0.89	5,320	642	0.76	16,800	...
20 days	-970	16.1	57	0.87	8,400	400	0.8	34,300	...
28 days	-880	10.4	28	0.91	9,100	546
35 days	-876	17.5	35	0.86	20,300	350
44 days	-854	11.2	36	0.85	31,500	322

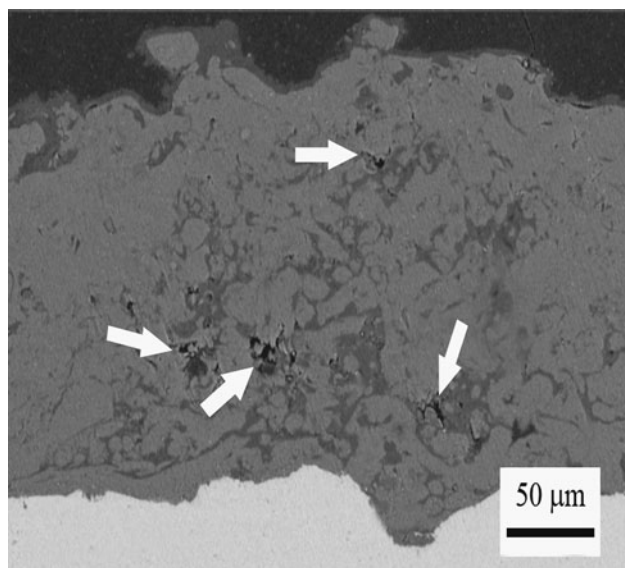


Fig. 8 SEM micrograph of the cross section of the coating after 44 days immersion in 3.5% NaCl solution. Arrows show attacked regions in the coating after immersion

39 at.% oxygen in the dark regions. These regions in the coating were formed during the corrosion process in the salt spray chamber.

To further illustrate the effects of barrier or pore resistance, the coated samples were analyzed by EIS after the accelerated exposure test. The spectra before and after exposure are presented in Fig. 11. The results showed that after 1500 h exposure, impedance values became higher which confirms that the effect of barrier or pore resistance could be significantly improved during exposure. This improvement is attributed to the pore sealing by corrosion products during exposure which is in a good agreement with statements reported by Rodriguez et al. (Ref 24).

Figure 12 shows the XRD pattern of the coating after 1500 h exposure. Identification of the peaks revealed that the phase composition of the surface of the coating is Al_2O_3 , aluminum hydrate, and pure aluminum. The existence of these oxide and hydrate impedes further penetration of the corrosive elements as they are compact and highly impervious.

According to the EIS measurements of the coating, anti-corrosion performance of the anodic coating can be improved by increasing the exposure time. This is due to the plugging of defects such as porosities, which are inherent characteristic of the thermally sprayed coatings (Ref 31). Plugging of defects occurs by the corrosion products which suppresses more penetration of the electrolyte into the coating. This could be the main reason for increasing the impedance values during exposure.

4. Conclusion

1. Thermally sprayed aluminum coatings can reliably protect steel structures against corrosion in

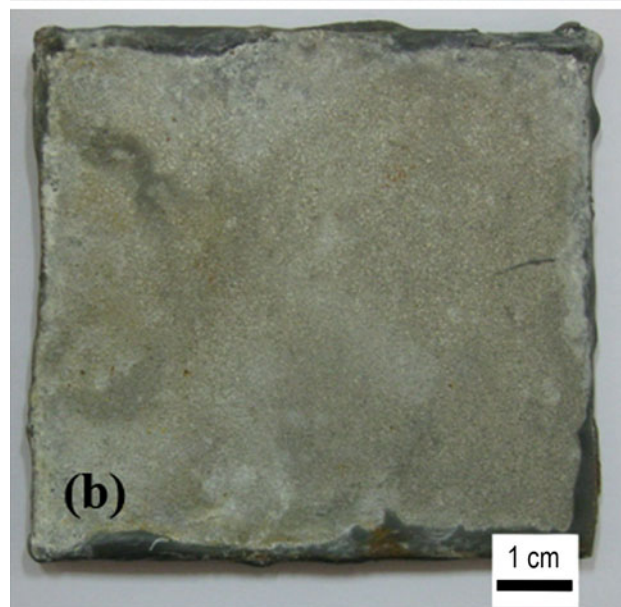
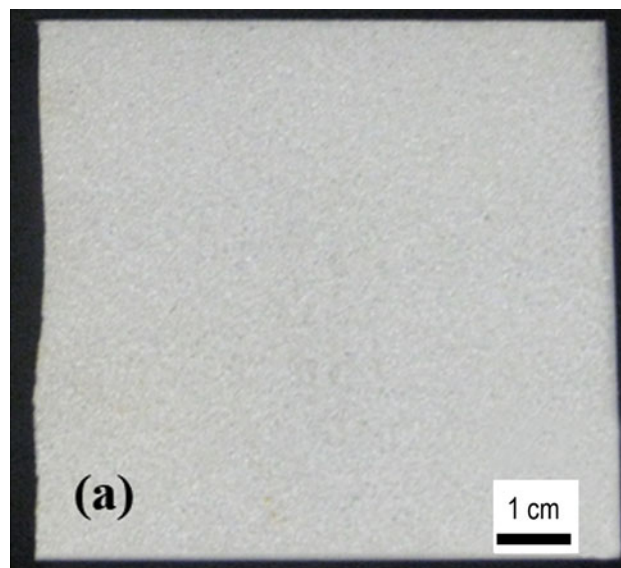


Fig. 9 Aluminum coating before (a) and after (b) 1500 h salt spray

chloride-containing aqueous solutions. Twin wire arc spray provides economical and operational (field use) advantages compared with other deposition processes which can be beneficial for coating complex and large steel structures.

2. Tafel polarization readings in 3.5% NaCl solution indicated that the current density of the arc sprayed aluminum coating is higher than that of the bulk aluminum which could be related to the existence of pores in the thermal spray coating. The electrolyte penetrated through the interconnected pores and reached the substrate and the current density of aluminum (less noble metal) accelerated due to the galvanic corrosion.



3. The EIS measurements showed that the penetration of the electrolyte through the coating defects affect the electrochemical behavior of the coatings during the exposure time. By increasing the exposure time, Warburg impedance observed for the coating indicated that the corrosion was strongly under diffusion control.
4. The EIS measurements also showed that the coatings performance can be improved by increasing the exposure time due to the plugging of defects by corrosion products which hinder higher penetration of the electrolyte through the porosities.
5. The EIS measurement after 1500 h salt spray test showed that the impedance values became higher

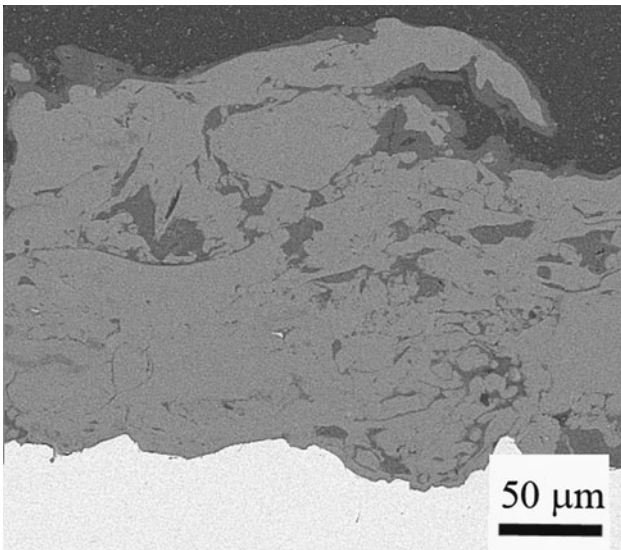
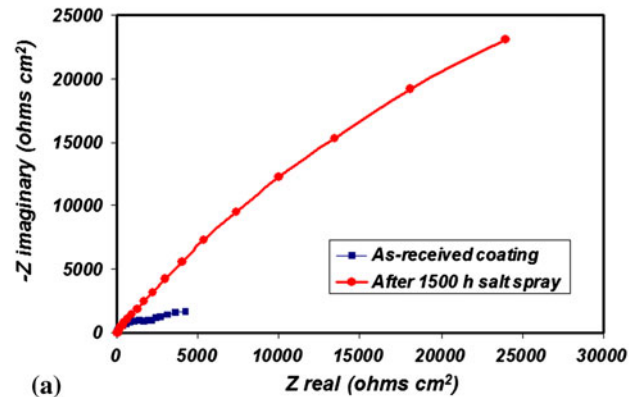
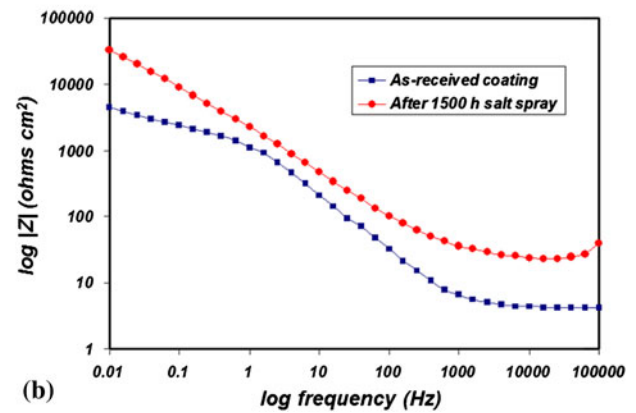


Fig. 10 The backscattered SEM micrograph of the cross section of aluminum coating after 1500 h exposure in a salt spray chamber

which confirm that the corrosion products act as barriers to the electrolyte penetration during exposure to salt spray. This improvement can be attributed to the pore sealing by corrosion products such as Al_2O_3 and $\text{Al}(\text{OH})_3$ during exposure.



(a)



(b)

Fig. 11 EIS Nyquist (a) and bode impedance (b) plots of aluminum coating before and after 1500 h exposure in a salt spray chamber

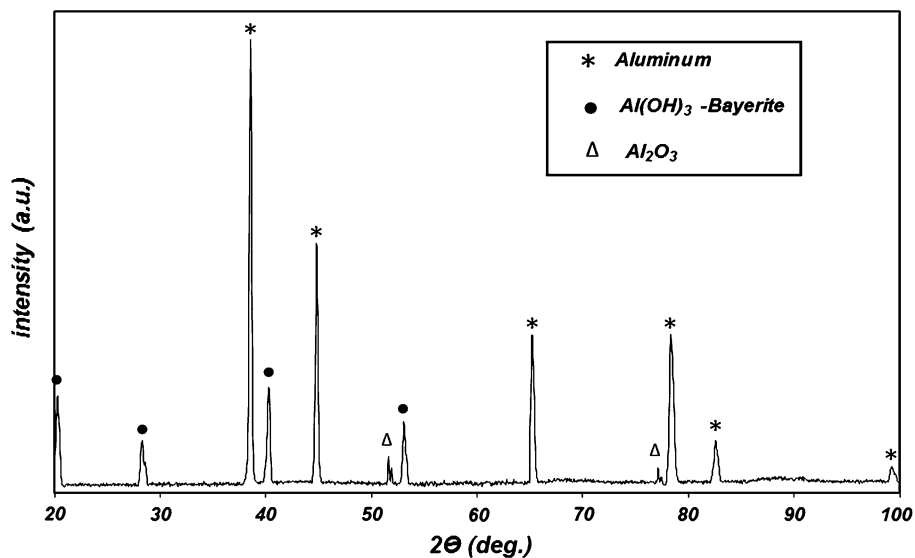


Fig. 12 XRD pattern of the aluminum sprayed coating after 1500 h salt spray

References

- N. Priyantha, P. Jayaweera, A. Sanjurjo, K. Laua, F. Lu, and K. Krist, Corrosion-Resistant Metallic Coatings for Applications in Highly Aggressive Environments, *Surf. Coat. Technol.*, 2003, **163-164**, p 31-36
- P. Novak, Anodic Protection, *Shreir's Corros.*, 2010, **4**, p 2857-2889
- C. Christodoulou, G. Glass, J. Webb, S. Austin, and C. Goodier, Assessing the Long Term Benefits of Impressed Current Cathodic Protection, *Corros. Sci.*, 2010, **52**, p 2671-2679
- A.R. Marder, The Metallurgy of Zinc-Coated Steel, *Prog. Mater. Sci.*, 2000, **45**, p 191-271
- E. Palma, J.M. Puente, and M. Morcillo, The Atmospheric Corrosion Mechanism of 55%Al-Zn Coating on Steel, *Corros. Sci.*, 1998, **40**, p 61-68
- A.B. Samui, A.S. Patankar, J. Rangarajan, and P.C. Deb, Study of Polyaniline Containing Paint for Corrosion Prevention, *Prog. Org. Coat.*, 2003, **47**, p 1-7
- A. Sakhri, F.X. Perrin, E. Aragon, S. Lamouric, and A. Benaboura, Chlorinated Rubber Paints for Corrosion Prevention of Mild Steel: A Comparison Between Zinc Phosphate and Polyaniline Pigments, *Corros. Sci.*, 2010, **52**, p 901-909
- R.P. Edavan and R. Kopinski, Corrosion Resistance of Painted Zinc Alloy Coated Steels, *Corros. Sci.*, 2009, **51**, p 2429-2442
- A. Guenbour, A. Benbachir, and A. Kacemi, Evaluation of the Corrosion Performance of Zinc-Phosphate-Painted Carbon Steel, *Surf. Coat. Technol.*, 1999, **113**, p 36-43
- S.A. Ali, H.A. Al-Muallem, S.U. Rahman, and M.T. Saeed, Bis-isoxazolidines: A New Class of Corrosion Inhibitors of Mild Steel in Acidic Media, *Corros. Sci.*, 2008, **50**, p 3070-3077
- D.Q. Zhang, Z.X. An, Q.Y. Pan, L.X. Gao, and G.D. Zhou, Comparative Study of Bis-piperidiniummethyl-urea and Mono-piperidiniummethyl-urea as Volatile Corrosion Inhibitors for Mild Steel, *Corros. Sci.*, 2006, **48**, p 1437-1448
- Z. Panossian, L. Mariaca, M. Morcillo, S. Flores, J. Rocha, J.J. Peña, F. Herrera, F. Corvo, M. Sanchez, O.T. Rincon, G. Pridyballo, and J. Simancas, Steel Cathodic Protection Afforded by Zinc, Aluminum and Zinc/Aluminum Alloy Coatings in the Atmosphere, *Surf. Coat. Technol.*, 2005, **190**, p 244-248
- O. de Rincon, A. Rincon, M. Sanchez, N. Romero, O. Salas, R. Delgado, B. Lopez, J. Uruchurtu, M. Marroco, and Z. Panosian, Evaluating Zn, Al and Al-Zn Coatings on Carbon Steel in a Special Atmosphere, *Constr. Build. Mater.*, 2009, **23**, p 1465-1471
- S.T. Vagge, V.S. Raja, and R. Ganesh Narayanan, Effect of Deformation on the Electrochemical Behavior of Hot-Dip Galvanized Steel Sheets, *Appl. Surf. Sci.*, 2007, **253**, p 8415-8421
- W.J. Smith and F.E. Goodwin, Hot Dipped Coatings, *Shreir's Corros.*, 2010, **4**, p 2556-2576
- L. Guzman, M. Adami, W. Gissler, S. Klose, and S. De Rossi, Vapour Deposited Zn-Cr Alloy Coatings for Enhanced Manufacturing and Corrosion Resistance of Steel Sheets, *Surf. Coat. Technol.*, 2000, **125**, p 218-222
- M.A. Baker, W. Gissler, S. Klose, M. Trampert, and F. Weber, Morphologies and Corrosion Properties of PVD Zn-Al Coatings, *Surf. Coat. Technol.*, 2000, **125**, p 207-211
- T. Sugama, CVD-Titanium Carbonitride Coatings as Corrosion-Preventing Barriers for Steel in Acid-Brine Steam at 200°C, *Mater. Lett.*, 1999, **38**, p 227-234
- C. Béguin, E. Horvath, and A.J. Perry, Tantalum Coating of Mild Steel by Chemical Vapour Deposition, *Thin Solid Films*, 1977, **46**, p 209-212
- G. Jandin, H. Liao, Z.Q. Feng, and C. Coddet, Correlations Between Operating Conditions, Microstructure and Mechanical Properties of Twin Wire Arc Sprayed Steel Coatings, *Mater. Sci. Eng., A*, 2003, **349**, p 298-305
- L. Pawlowski, *The Science and Engineering of Thermal Spray Coatings*, 2nd ed., John Wiley & Sons Ltd, West Sussex, 2008
- M.S. Han, Y.B. Woo, S.C. Ko, Y.J. Jeong, S.K. Jang, and S.J. Kim, Effects of Thickness of Al Thermal Spray Coating for STS 304, *Trans. Nonferrous Met. Soc. China*, 2009, **19**, p 925-929
- D. Chaliampalias, G. Vourlias, E. Pavlidou, G. Stergioudis, S. Skolianos, and K. Chrissafis, High Temperature Oxidation and Corrosion in Marine Environments of Thermal Spray Deposited Coatings, *Appl. Surf. Sci.*, 2008, **255**, p 3104-3111
- R.M. Rodriguez, R.S.C. Paredes, S.H. Wido, and A. Calixto, Comparison of Aluminum Coatings Deposited by Flame Spray and by Electric Arc Spray, *Surf. Coat. Technol.*, 2007, **202**, p 172-179
- D.P. Schmidt, B.A. Shaw, E. Sikora, W.W. Shaw, and L.H. Laliberte, Corrosion Protection Assessment of Sacrificial Coating Systems as a Function of Exposure Time in a Marine Environment, *Prog. Org. Coat.*, 2006, **57**, p 352-364
- L.M. Liu, Zh Wang, and G. Song, Study on Corrosion Resistance Properties of Hydrothermal Sealed Arc Sprayed Aluminum Coating, *Surf. Eng.*, 2010, **26**, p 399-406
- Norma Nace RM01 70, Visual Standard for Surfaces of New Steel Airblast. Cleaned with Sand Abrasive-(item # 53005), 1970
- "Standard Test Method for Adhesion or Cohesion Strength of Thermal Spray Coatings," ASTM Standard C 633-01, ASTM, West Conshocken, PA, USA, 2001
- ASTM B 117/90: Standard Test method of Salt Spray (FOG) Testing, 1990, p 19
- K. Spencer, D.M. Fabijanac, and M.X. Zhang, The Use of Al-Al₂O₃ Cold Spray Coatings to Improve the Surface Properties of Magnesium Alloys, *Surf. Coat. Technol.*, 2009, **204**, p 336-344
- M. Campo, M. Carboneras, M.D. López, B. Torres, P. Rodrigo, E. Otero, and J. Rams, Corrosion Resistance of Thermally Sprayed Al and Al/SiC Coatings on Mg, *Surf. Coat. Technol.*, 2009, **203**, p 3224-3230
- P.H. Suegama, C.S. Fugivara, A.V. Benedetti, J. Fernández, J. Delgado, and J.M. Guilemany, Electrochemical Behavior of Thermally Sprayed Stainless Steel Coatings in 3.4% NaCl, *Corros. Sci.*, 2005, **47**, p 605-620
- E. Celik, I. Ozdemir, E. Avci, and Y. Tsunekawa, Corrosion Behavior of Plasma Sprayed Coatings, *Surf. Coat. Technol.*, 2005, **193**, p 297-302
- M.M. Verdian, K. Raeissi, and M. Salehi, Corrosion Performance of HVOF and APS Thermally Sprayed NiTi Intermetallic Coatings in 3.5% NaCl Solution, *Corros. Sci.*, 2010, **52**, p 1052-1059
- D. Yang, C. Liu, X. Liu, M. Qi, and G. Lin, EIS Diagnosis on the Corrosion Behavior of TiN Coated NiTi Surgical Alloy, *Curr. Appl. Phys.*, 2005, **5**, p 417-421
- C. Liu, Q. Bi, and A. Matthews, EIS Comparison Performance of PVD TiN and CrN Coated Mild Steel in 0.5 N NaCl Aqueous Solution, *Corros. Sci.*, 2001, **43**, p 1953-1961
- C. Liu, Q. Bi, A. Leyland, and A. Matthews, An Electrochemical Impedance Spectroscopy Study of the Corrosion Behavior of PVD Coated Steels in 0.5 N NaCl Aqueous Solution: Part I. Establishment of Equivalent Circuits for EIS Data Modeling, *Corros. Sci.*, 2003, **45**, p 1243-1256
- M.M. Verdian, K. Raeissi, and M. Salehi, Electrochemical Impedance Spectroscopy of HVOF-Sprayed NiTi Intermetallic Coatings Deposited on AISI, 1045 Steel, *J. Alloys Compd.*, 2010, **507**, p 42-46
- S.H. Ahn, Y.S. Choi, J.G. Kim, and J.G. Han, A Study on Corrosion Resistance Characteristics of PVD Cr-N Coated Steels by Electrochemical Method, *Surf. Coat. Technol.*, 2002, **150**, p 319-326
- Y. Wang, W. Tian, T. Zhang, and Y. Yang, Microstructure, Spallation and Corrosion of Plasma Sprayed Al₂O₃-13%TiO₂ Coatings, *Corros. Sci.*, 2009, **51**, p 2924-2931